Chemical Methodologies 4(2020) 514-531

Chemical Methodologies

Journal homepage: http://chemmethod.com

Original Research article

Theoretical Study of the Reaction Among Isocyanide, Dialkyl Acetylenedicarboxylate and Acetic Anhydride: The Investigation of the Reaction

Batoul Makiabadi[a], Mohammad Zakarianezhad* [b], Fahimeh Koorkinejad[b], Hoseyn Mehdizadeh[b]

[a] Department of Chemical Engineering, Sirjan University of Technology, Sirjan, Iran

[b] Department of Chemistry, Payame Noor University, Tehran, Iran

ARTICLE INFORMATION

Received: 04 November 2019
Received in revised: 13 January 2020
Accepted: 12 April 2020
Available online: 01 July 2020

DOI: 10.33945/SAMI/CHEMM.2020.4.11

KEYWORDS

Theoretical study
Alkyl isocyanides
[2+3] Cycloaddition
Reaction mechanism

ABSTRACT

In this work, stepwise reaction mechanism of the [2+3] cycloaddition reaction among alkyl isocyanides (contains *tert*-butyl isocyanide, cyclo hexyl isocyanide) with dialkyl acetylenedicarboxylate (contains dimethyl acetylenedicarboxylate, diethyl acetylenedicarboxylate and di-*tert*-butyl acetylenedicarboxylate) at the presence of acetic anhydride was investigated both in the gas phase and in solvent was studied theoretically. The potential energy of all structures participated in the reaction path was evaluated. The geometry of all the structures participated during the reaction path, the rate-determining step, and potential competitive routes during the reaction coordinate were evaluated. Also, dielectric constant effect of the solvent, the effect of substituted alkyl groups on the potential energy surfaces, and the best product configuration were investigated based upon the quantum mechanical calculations. For better understanding of the molecular interaction, the natural bond orbital method (NBO) and AIM analysis were applied. The results indicated that, the first step of the reaction was recognized as rate-determining step and the reaction rate was predicted to be dependent on the concentration of alkyl isocyanides and dialkyl acetylenedicarboxylate. It was also found that, the electron donating of different alkyl groups was not the main factor for the variation in the potential energy surfaces of the reaction; however, the steric factor of the bulky alkyl groups participating in the reaction path was found to be the main factor.

*Corresponding author: E-mail: (m.zakarianejad@yahoo.com), (mzakarianejad@pnu.ac.ir), Department of Chemistry, Payame Noor University, Tehran, Iran, Tel: +983455233540

Graphical Abstract

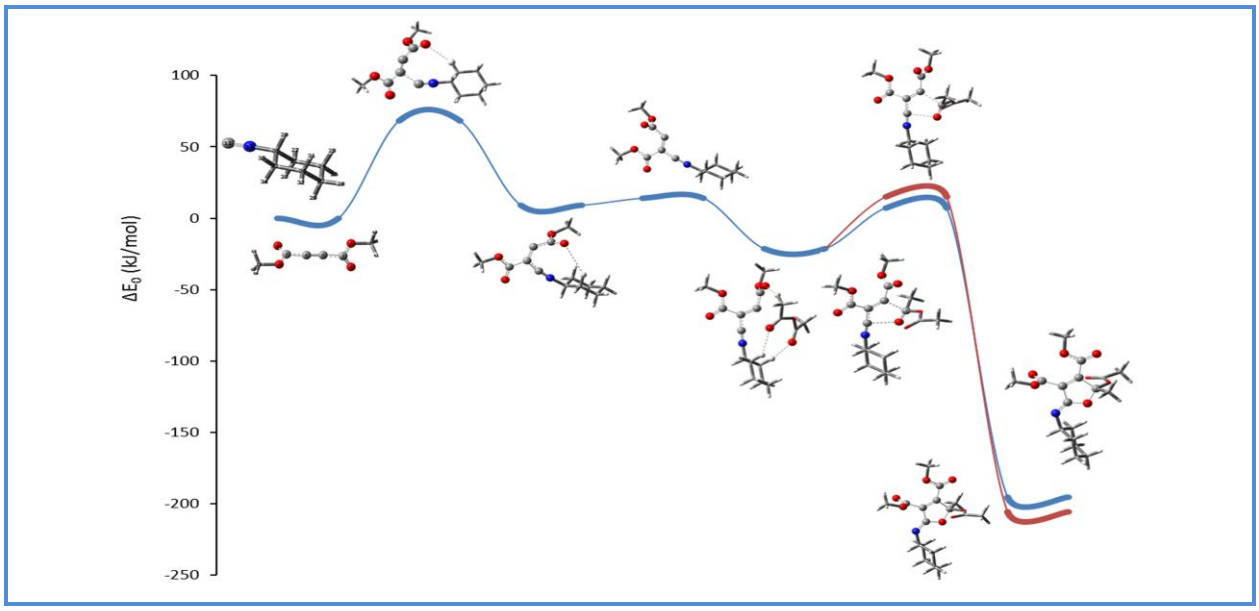

Introduction

In recent years, multi-component reactions (MCRs) because of atom economy, conversion character, and simplicity in a one pot operation are interest due to their ability to generate highly complex final products [1]. These reactions with significant structural diversity are efficient in the synthesis of drugs, which isocyanide based multicomponent reactions (IMCR) play an important role in this field. Isocyanides compounds are important materials in chemistry and many of them have found general application in organic synthesis [2]. An isocyanide is an organic compound with -N≡C functional group which connected to the organic fragment *via* the nitrogen atom. Alkyl isocyanides are used as the important mediate in the synthesis of a wide range of compounds. Isocyanides are reactants in many multicomponent reactions of interest in organic synthesis, two of which are: the Ugi reaction [3] and the passerini reaction [4]. Furans are one of the most important compounds in organic chemistry. Many of furan products show inspiring biological activities, such as cytotoxic and antitumor properties, antispasmodic, anti-feeding and antimicrobial activities [5]. Polysubstituted furans are used in synthesis of natural and no natural products. Therefore, the effort to synthesize of these materials is of great value. Polysubstituted furans, various annulated derivatives such as benzo, thieno, isoxazolo, furo, pyridino, pyridazino, and indolofuran have been synthesized and their properties investigated [6]. Furans are useful synthetic intermediates [7–9] finding utility as masked a, *b*-unsaturated esters [10], and as precursors to hydroxypyranones [11] and

polyoxygenated natural products [12] as well as two mono and oligosaccharides [13]. Furan substructures are an important motif in materials chemistry providing promising plastics derived from renewable sources [14], self-healing macromolecular materials [15], conducting polymers [16], and photovoltaics [17]. Hence, the synthesis of furans has attracted considerable attention [18, 19]. Isocyanides undergo a formal [2+3] cycloaddition reaction with conjugated electrophilic heterocyclic five-membered ring systems [20]. In this reaction, after formation of a zwitterionic intermediate, the reaction proceeds *via* a stepwise [2+3] cycloaddition in the presence of acetic anhydride (Figure 1). Quantum mechanical calculations were performed to gain a better understanding of the most important geometrical parameters. Also, to determine different parameters affecting the reaction mechanism and determining the effect of different substituted groups on the potential energy surfaces, the reaction mechanism was evaluated in details.

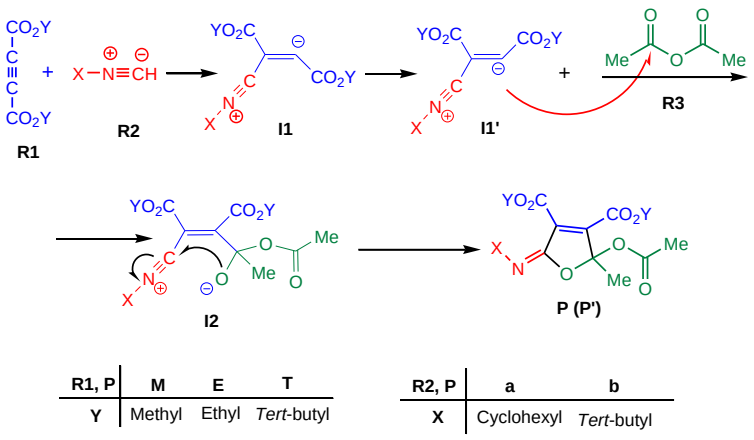

Figure 1. The reaction among dialkyl acetylenedicarboxylate (R1), alkyl isocyanide (R2) and acetic anhydride (R3) affording the product P(P')

Possible reaction mechanisms include nuleophilic attack of the atom C11 of alkyl isocyanide (R2) to the atom C6 of dialkyl acetylenedicarboxylate (R1), *via* passing from transition state of Ts1, to form the zwitter ion of intermediate I1 which turns into the intermediate I1'. Intermediate I2 formed from interaction between I1' and third reactant (acetic anhydride) (R3), which through a [2+3] addition-cyclization process, with passing *via* transition state TS2 (TS2'), ends to the two products P (P'), respectively (Figures 1 and 2).

Experimental

Computational methods

All the structures in this work were optimized with B3LYP.6-311++G (d,p) level using Gaussian 09 and Gamess suite software package [21, 22]. Vibrational frequencies were obtained at the same level for characterization of stationary points and thermal zero-point energy corrections. Intrinsic reaction coordinate (IRC) approach [23-26] was performed to ensure that the given transition state connects with the corresponding reactants and products. Calculations have been carried out both in the gas phase and in solvent (acetone and dichloromethane) with PCM model [27-29]. The natural bond orbital (NBO) analysis was carried out at 6-311++G (d,p) level of theory using version 3.1 of NBO package [30]. In addition, topological properties were calculated using AIM methodology on the wave functions obtained at 6-311++G (d,p) level [31].

Investigation of the reaction between dialkyl acetylenedicarboxylate (DAAD) (R1) and alkyl isocyanide (R2) in the presence of acetic anhydride

Potential energy levels in gas phase

The optimized geometries of all structures are included in Figures 2 and 3. Also, the potential energy level for all the structures participated in the reaction mechanism in all pathways are presented in Figures 4 and 5. Reaction mechanism of dimethyl acetylene dicarboxylate (DMAD) (R1-M) with cyclohexyl isocyanide (R2a) in the presence of acetic anhydride (R3) includes two activation barriers of TS1a-M and TS2a-M (TS2′a-M) (Figure 4). The first and second energy barriers are equal to 68.2 kJ/mol and 28.4 kJ/mol (29.3 kJ/mol), respectively. This indicates 39.8 kJ/mol (38.9 kJ/mol) reduction of the second step energy barrier compared to the first step. Comparing these two energy barriers in the competitive paths in the second step, can be concluded that the first competitive path is slightly more stable with a value of 0.9 kJ/mol in comparison with the second competitive path. Therefore, there is not any special kinetics preference between these two competing pathways. Stability of the ultimate product of the reaction in the second competitive path a'-M (Pa'-M) was only 2.3 kJ/mol compared with that of the first competitive path a-M (Pa-M). Therefore, there was not any detectable thermodynamic stability in these two pathways. The total reaction had a relative Gibbs free energy of -78.4 kJ/mol (-81.3 kJ/mol) and relative enthalpy of -201.3 kJ/mol (-203.5 kJ/mol) which is spontaneous and exothermic. According to the results, the rate-determining step is the first step of the reaction mechanism.

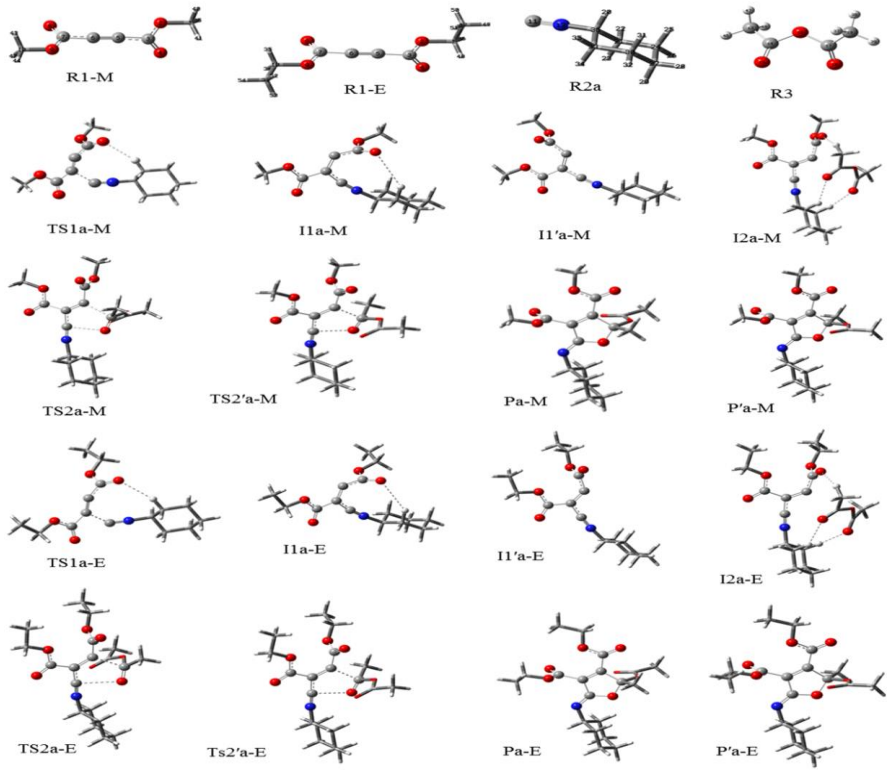

Figure 2. Optimized geometries of all structures in the pathways a-M and a-E of the reaction

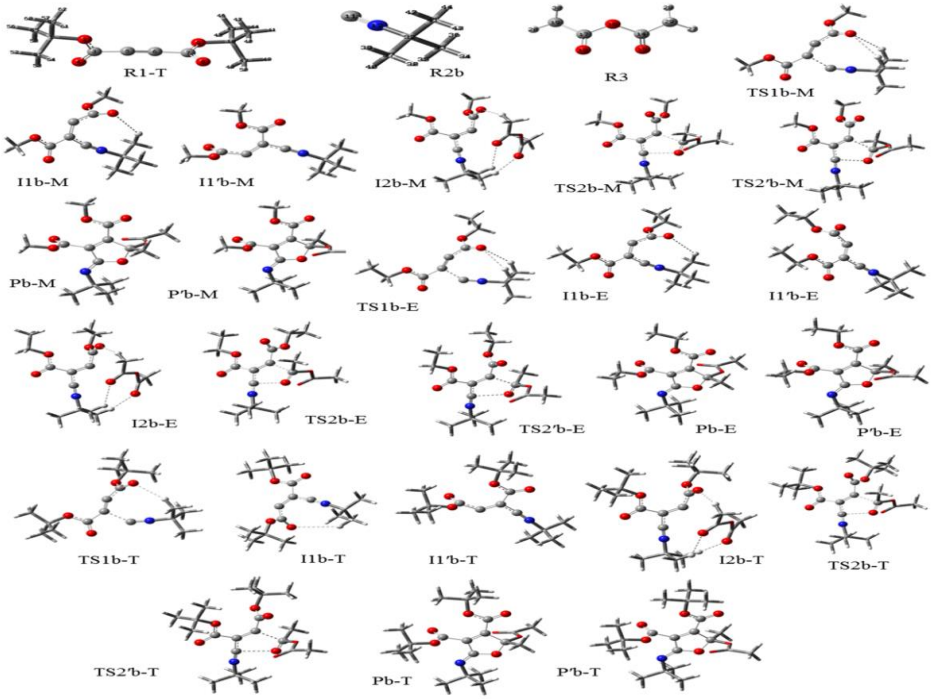

Figure 3. Optimized geometries of all structures in the pathways b-M, b-E and b-T of the reaction

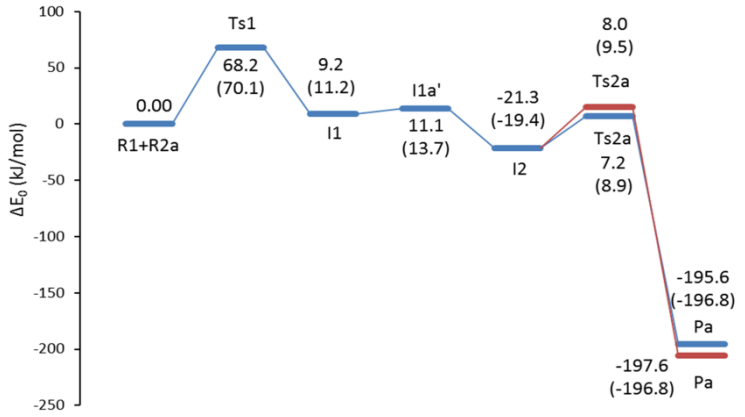

Figure 4. The potential energy profile of the reaction in two paths a-M and a-E (data of the path a-E are in parentheses)

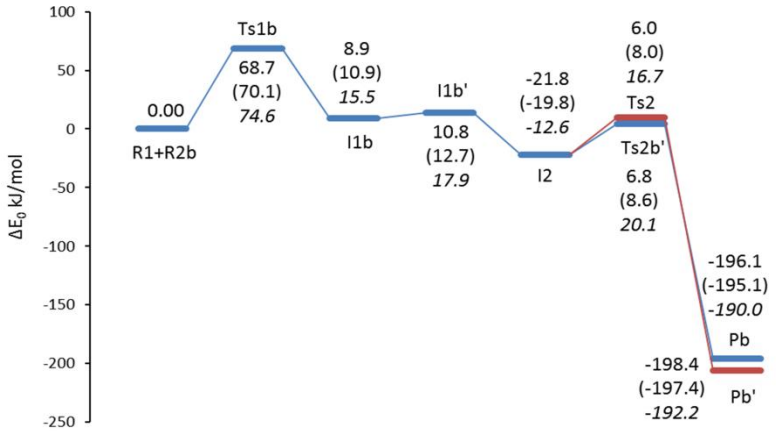

Figure 5. The potential energy profile of the reaction in paths b-M, b-E and b-T (data of the path b-E are in parentheses and data of the path b-T are in italic form)

Two activation energy barriers of TS1a-E and TS2a-E (TS2a'-E) in the presence of diethyl acetylene dicarboxylate (DEAD) (R1-E), R2a and R3 are 70.1 kJ/mol and 28.3 kJ/mol (28.9 kJ/mol), respectively, which as same as the previous pathway indicates a reduction of 41.8 kJ/mol (41.3 kJ/mol) of the second step energy barrier in comparison to the first one. In the second step of the reaction, the two competitive pathways with only 0.6 kJ/mol difference, no specific kinetic preference was observed. The stability of the final reaction product in the competitive path a'-E (Pa'-E) in comparison to the competitive path a-E (Pa-E) is just 2.2 kJ/mol, therefore, no specific thermodynamic stability was observed in the two competitive pathways. The total reaction has a relative Gibbs free energy of -76.4 kJ/mol (-78.8 kJ/mol) and relative enthalpy of -200.5 kJ/mol (-202.7 kJ/mol) which is indicative of a spontaneous and exothermic reaction. Regarding to the results, the first step of the reaction has also determined as rate-determining step. The two activation energy barriers of TS1b-M, and TS2b'-M in the

presence of dimethyl acetylene dicarboxylate (R1-M), *tert*-butyl isocyanid (R2b) and R3 were 68.7 kJ/mol and 27.8 kJ/mol (28.6 kJ/mol), respectively, which illustrates a decrease in the second step energy barrier compared to the first one with a value of 40.8 kJ/mol (40.1 kJ/mol). The stability of the product of the reaction in the competitive path b'-M (Pb'-M) was only 2.3 kJ/mol compared to the competitive path b-M (Pb-M). Therefore, there was not any detectable thermodynamic stability in these two pathways. The total reaction had a relative Gibbs free energy of -79.8 kJ/mol (-82.5 kJ/mol) and relative enthalpy of -202.1 kJ/mol (-204.3 kJ/mol) which was spontaneous and exothermic. According to the results, the first step of the reaction mechanism was the rate-determining step. In the presence of R1-E, R2b and R3, the two activation energy barriers of the reaction, TS1b-E and (TS2b'-E) TS2b-E, were 70.1 kJ/mol and 27.8 kJ/mol (28.4 kJ/mol) which indeed demonstrates that the energy barrier of the second step is diminished with a value of 42.2 kJ/mol (41.7 kJ/mol) in comparison to the first step. Stability of the final reaction product in the second competitive path (P'b-E) was just 2.2 kJ/mol more than that of the first competitive path b-E (Pb-E), so any particular thermodynamic stability was not observed. The relative Gibbs free energy and the relative enthalpy of the overall reaction were -77.5 kJ/mol (-80.1 kJ/mol) and -201.2 kJ/mol (-203.5 kJ/mol), respectively, which indicated that the overall reaction was exothermic and spontaneous. According to the results, at the presence of di-*tert*-butyl acetylenedicarboxylate (R1-T) with R2b and R3, two activation energy barriers of the reaction, TS1b-T and TS2b-T (TS2b'-T), were 74.6 kJ/mol and 29.2 kJ/mol (32.6 kJ/mol), respectively, indicating that the energy barrier of the second step was 45.4 kJ/mol (42 kJ/mol) less than that of the first step. Results indicate that no particular kinetic preference and no particular thermodynamic stability were also observed. The relative Gibbs free energy and the relative enthalpy of the overall reaction were -70.6 kJ/mol (-72.8 kJ/mol) and -196 kJ/mol (-198.2 kJ/mol), respectively that indicate that the overall reaction is exothermic and spontaneous. Comparing two activation energy barriers of reaction shows that in the presence of R2a and R1-E reactants, the first activation energy barrier of reaction mechanism is increased slightly (1.9 kJ/mol) compared to the barrier of reaction in the presence of R2a and R1-M and the second energy barrier also was increased slightly (1.7 kJ/mol (1.4 kJ/mol)) and the final products of Pa-M (Pa'-M) are more stable, more spontaneous and more exothermic than the final products of Pa-E (Pa'-E). In addition, following the studies on the activation energy barriers of the reaction, it is indicated that the first and second activation energy barriers of the reaction are slightly increased in the presence of R1-M and R2b reactants (1.4 kJ/mol and 1.8 kJ/mol). The value of this increase in the energy barriers in the presence of R1-T and R2b will be more significant (6 kJ/mol and 7.7 kJ/mol (13.2 kJ/mol)). Studies revealed that the final product is more unstable and nonspontaneous, in going from Pb-M (Pb'-M) to Pb-T (Pb'-T) and the extent of exothermicity was reduced. Considering

the results, the value of the energy barrier increase in the presence of R1-T is more than R1-E. The highest energy barrier and most unstable product is assigned to the product of the reaction between R1-T and R2b and the most stable, spontaneous and exothermic product attributes to the product of Pb-M. Furthermore, in all mechanisms of the reaction the ultimate product in the second competitive paths (a' and b') is more stable than the one in the first step (a and b). When the results from the reaction between R1-M and R2a (R2b) are compared, it is indicated that the activation energy barrier of the first step of the reaction in the presence of R2a is slightly (0.5 kJ/mol) lower than the activation energy barrier of the first step in the presence of R2b, while the second activation energy barrier of the reaction with R2a is slightly more (1.2 kJ/mol) than the reaction in the presence of R2b. Finally, the final product of the reaction Pb-M (Pb'-M) is a little more stable by the values of 0.8 (0.8 kJ/mol) compared to the of Pa-M (Pa'-M).

The obtained results from the reaction between R1-E and R2a (R2b) illustrates that the activation energy barrier of the first step of the reaction with R2a is equal to the one in the presence of R2b reactant (70.1 kJ/mol). Comparison of the second activation energy barrier of the reaction indicates that the activation energy barrier of the reaction with R2a is slightly more (0.9 kJ/mol) than the activation energy with the R2b. Ultimately, the products Pb-E (Pb'-E) is also slightly more stable than the product of Pa-E (Pa'-E), by the value of 0.6 (0.6 kJ/mol). Results show that the strict effects of the alkyl group in the structure of dialkyl acetylene dicarboxylate and isocyanide can be considered as the main and important factor of the difference in the potential energy of some structures. Detailed investigations suggest that in the reaction between R2a and R1M (R1-E), the potential energy levels of the resulting structures after the reaction in the presence of R1-M decrease in comparison to the case in which R1-E is used. This reduction in the structures of I1a-M and I1′a-M is considerable. In addition, comparison of the potential energy levels for the reaction between R2b and R1-M, R1-E and R1-T) indicates that the potential energy levels of the resulting structures from the reaction increase in going from R1-M to R1-T which this increase is considerable in TS2b-T, TS2b'-T and I2b-T. The first activation barrier of the reaction with R1-E and R2a rose to some extent compared to the case in which R1-M and R2a is used, but the activation energy barrier of the second step slightly increased (1.7 kJ/mol and 1.4 kJ/mol). An increase in the energy barrier of the first step is caused by the instability of TS1a-E compared to TS1a-M with a value of 1.9 kJ/mol. Increasing the second step energy barrier at the presence of the R1-E was due to the higher instability of the potential energy level of TS2a-E in comparison to the I2a-E structure. The first activation energy of the reaction in the presence of R1-E and R2b slightly increased (1.4 kJ/mol) rather than the reaction in the presence of R1-M and R2b. The increase of the activation barrier in the presence of R1-T was more considerable (6 kJ/mol). Increase of the energy barrier in the

presence of R1-E and R1-T is due to the instability of TS1b-E and TS1b-T compared to TS1b-M with the amount of 1.4 kJ/mol and 6 kJ/mol, respectively. The second activation energy barrier of this reaction in the presence of R1-E slightly increased (2 kJ/mol and 1.7 kJ/mol) with respect to R1-M, this is attributed to the higher increase of potential energy level of TS2b-E (TS2b'-E) compared to I2b-E. The second activation barrier of the reaction in the presence of R1-T and R2b rose in comparison to the reactions with R1-M and R2b, by the value of 10.6 kJ/mol (13.2 kJ/mol). The increase in the energy barrier of the second step in the presence of R1-T is caused by the higher instability of TS2b-T with respect to I2b-T structure.

Energy in aqueous phase

In order to investigate the effect of solvent on the potential energy surfaces, all the structures in the aqueous phase were optimized in the presence of dichloromethane and acetone solvents with dielectric constants of 8.93 and 20.49, respectively. Optimization of structures in aqueous phase was performed only in cases with the reaction between R1-M and R2b. The potential energy level for all the structures in this reaction path (b-M) are presented in Figure 5. The obtained results in dichloromethane indicates that the potential energy surface of all the participated structures in the reaction mechanism, except I1b-M and I1b'-M, increased significantly with respect to gas phase. In acetone, the potential energy level of all participating structures in the reaction mechanism, except TS1b-M and Pb-M (Pb'-M), reduced compared with that of the gas phase. Comparison of the potential energy levels in both dichloromethane and acetone solvents illustrate a decrease in the potential energy level of all structures in acetone solvent compared to dichloromethane. The first activation energy barrier of the reaction in dichloromethane increased slightly (3.5 kJ/mol) compared to the gas phase. The increase in the first energy barrier is due to the instability of the potential energy level of TS1b-M structure in comparison to the gas phase with a value of 3.5 kJ/mol. The second activation energy barrier of the reaction in the first competitive path (TS2b-M) slightly increases (1.8 kJ/mol) and this increase is caused by the higher instability of the TS2b-M with respect to I2b-M in dichloromethane solvent. This energy barrier in the second competitive path (TS2b'-M) diminishes to a lower extent (0.6 kJ/mol). This reduction is caused by the higher stability of TS2b'-M than I2b-M in dichloromethane. Relative enthalpy (ΔH) and relative Gibbs free energy (ΔG) of the total reaction is -176.8 kJ/mol (-177.6 kJ/mol) and -54.4 kJ/mol (-55.7 kJ/mol), respectively and indicates that the total reaction is exothermic and spontaneous. In order to investigate the effect of dielectric constant of the solvent on the potential energy levels and the reaction mechanism, all the structures were optimized in acetone with dielectric constant of 20.49. The presented results in Figure 6 illustrates that the electronic energy of all the participant structures in the

reaction mechanism in acetone solvent encounters a significant reduction compared to dichloromethane solvent. In intermediate structures, the highest level of decrease in electronic energy takes place. Investigation of results for acetone solvent signifies that the first energy barrier slightly diminishes (1.1 kJ/mol) compared to dichloromethane and the second energy barrier encountered an increase to lower extent (1 kJ/mol and 0.2 kJ/mol). Compared to gas phase, the first energy barrier slightly increases (2.4 kJ/mol) and the increase of the first energy barrier is related to the instability of TS1b-M with a value of 2.4 kJ/mol in acetone solvent with respect to the gas phase, but the competitive pathway represents a dual behavior. The second energy barrier in the first competitive path, increased to a value 2.8 kJ/mol compared to the gas phase, which is due to the higher instability of TS2b-M structure with respect to I2b-M in the acetone. The second competitive path (TS2b'-M) encounters a decrease 0.5 kJ/mol which suggests that the TS2b'-M structure is more stable than the I2b-M in acetone solvent. In acetone solvent, the reaction is exothermic and spontaneous in which the relative enthalpy (ΔH) and Gibbs free energy change (ΔG) of the total reaction is -174.7 kJ/mol (-175 kJ/mol) and -52.3 kJ/mol (-53.2 kJ/mol), respectively.

Values of the dipole moment (μ) of the participating structures in the reaction mechanism in gas phase and in the presence of dichloromethane and acetone solvents are presented in Table 1. As can be seen, by increasing the polarity of the solvent, the electronic energy of structures reduced. The induced effect of the polar solvents leads to an increase in the dipole moment of the structures. When the value of dipole moment is higher, the interaction between the solvent and solute increases and as a result the stability of the structure enhances. Studying the results indicates that structures with high dipole moment values possess higher stability in the presence of solvent. Upon raising the dielectric constant of the solvent (ε), the extent of stability also increased.

Table 1. Dipole moment values (μ/D) of all structures participating in the reaction mechanism both in the gas phase and in solution

structure	gas phase	acetone	dichloromethane	structure	gas phase	acetone	dichloromethane
R1-T	2.6143	3.2921	3.3845	I2b-T	2.2968	4.5933	7.0871
R2b	4.1216	5.0805	5.1923	TS2b-T	2.8456	3.905	4.0343
R3	3.9806	5.1743	5.3349	Pb-T	2.914	4.0371	4.2571
TS1b-T	3.1549	5.3815	5.5765	TS2'b-T	2.7723	8.3504	8.7503
I1b-T	5.9947	8.8853	9.2134	P'b-T	1.8675	2.4647	2.5597
I1'b-T	6.6301	8.7645	8.9983				

To obtain more detailed information, the strength and nature of the hydrogen bonds, analysis of the electron density ρ(r) in bond critical points, laplacian of the electron density ($\nabla^2\rho$(r)) and the total

electron density H(r) in bond critical points (BCPs) for structures in the pathway a-M are calculated using the theory of atoms in molecules and the results are presented in Table 2.

Table 2. Values of the electron density ρ(r) in bond critical points, laplacian of the electron density ($\nabla^2\rho$(r)) andthe total electron density H(r) in the pathway a-M of the reaction

structure	Bond	ρ(r)	$\nabla^2\rho$(r)	H(r)	structure	Bond	ρ(r)	$\nabla^2\rho$(r)	H(r)
Ra-M	C6-C5	0.406	-1.206	-0.578	TS2a-M	C6-C5	0.326	-0.914	-0.359
	N12-C11	0.430	-0.010	-0.723		C11-C6	0.277	-0.739	-0.303
TS1a-M	C6-C5	0.383	-1.122	-0.509		N12-C11	0.456	0.036	-0.796
	C11-C6	0.085	0.046	-0.025		O15-C11	0.015	0.054	0.002
	N12-C11	0.437	0.068	-0.743	TS2'a-M	C6-C5	0.326	-0.914	-0.359
I1a-M	C6-C5	0.319	-0.874	-0.349		C11-C6	0.277	-0.738	-0.302
	C11-C6	0.277	-0.706	-0.312		N12-C11	0.456	0.038	-0.796
	N12-C11	0.444	-0.028	-0.764	Pa-M	C6-C5	0.339	-0.979	-0.383
I1'a-M	C6-C5	0.321	-0.895	-0.351		C11-C6	0.273	-0.695	-0.244
	C11-C6	0.279	-0.731	-0.326		N12-C11	0.398	-1.057	-0.629
	N12-C11	0.446	-0.037	-0.770	P'a-M	C6-C5	0.339	-0.979	-0.383
I2a-M	C6-C5	0.322	-0.895	-0.352		C11-C6	0.273	-0.694	-0.244
	C11-C6	0.278	-0.736	-0.317		N12-C11	0.398	-1.056	-0.629
	N12-C11	0.450	-0.002	-0.780					

Analysis of the participating atoms in the reaction mechanism in gas phase and the important transitions in the involved bonds is performed using NBO software, including charge transfer energy and natural charge in the gas phase is summarized in Tables 3 and 4.

Table 3. NBO results in the pathways a-M and a-E of the reaction

	R1-M	R2a	R3	TS1a-M	I1a-M	I1'a-M	I2a-M	TS2a-M	TS2'a-M	Pa-M	P'a-M
q_{C5}	-0.008			-0.133	-0.415	-0.422	-0.117	-0.007	-0.011	-0.127	-0.125
q_{C6}	-0.034			-0.057	-0.007	-0.068	-0.412	-0.390	-0.389	-0.042	-0.042
q_{C11}		0.258		0.403	0.621	0.652	0.656	0.690	0.690	0.558	0.558
q_{N12}		-0.530		-0.432	-0.308	-0.313	-0.283	-0.249	-0.248	-0.456	-0.457
q_{C14}			0.821				0.834	0.756		0.583	
q_{O15}			-0.530				-0.566	-0.695	-0.695	-0.576	
CT				0.272				-0.309	-0.309		
	R1-E	**R2a**	**R3**	**TS1a-E**	**I1a-E**	**I1'a-E**	**I2a-E**	**TS2a-E**	**TS2'a-E**	**Pa-E**	**P'a-E**
q_{C5}	-0.020			-0.138	-0.414	-0.422	-0.117	-0.010	-0.124	-0.014	-0.122
q_{C6}	-0.020			-0.055	-0.009	-0.068	-0.411	-0.390	-0.051	-0.388	-0.051
q_{C11}		0.260		0.405	0.621	0.654	0.656	0.690	0.561	0.690	0.561
q_{N12}		-0.532		-0.432	-0.310	-0.315	-0.285	-0.251	-0.458	-0.250	-0.459
q_{C14}			0.821				0.835	0.757	0.583		
q_{O15}			-0.530				-0.567	-0.694	-0.577		
CT				0.273				-0.307	-0.307		

Charge analysis in DAAD illustrates that DEAD and DTAD structures are completely symmetric but in DMAD the molecular symmetry is not maintained. The asymmetry in this structure results inequality of the atomic charge in C5 and C6 atoms. Comparison of atomic charges in R2a and R2b

structures indicate that in all structures, the charge of C11 atom is almost the same. With these results it expected that no specific preference observed in the nucleophilic attack of C11 to C6 atom in these structures. Investigations illustrates that the potential energy level in transition state structures TS1a-M, TS1a-E, TS1b-M, TS1b-E and TS1b-T do not show any significant variation. Small variations in the energy level may be due to the presence of substituted bulk groups in these structures.

Table 4. NBO results in the pathways b-M, b-E and b-T of the reaction

	R1-M	**R2b**	**R3**	**TS1b-M**	**I1b-M**	**I1'b-M**	**I2b-M**	**TS2b-M**	**TS2'b-M**	**Pb-M**	**P'b-M**
q_{C5}	-0.027			-0.135	-0.419	-0.423	-0.117	-0.007	-0.146	-0.0113	-0.124
q_{C6}	-0.012			-0.056	-0.007	-0.067	-0.412	-0.389	-0.313	-0.388	-0.048
q_{C11}		0.257		0.406	0.623	0.655	0.656	0.690	1.971	0.6903	0.565
q_{N12}		-0.547		-0.448	-0.327	-0.330	-0.300	-0.268	-1.048	-0.268	-0.475
q_{C14}			0.821				0.834	0.755	0.550		
q_{O15}			-0.530				-0.564	-0.695	-0.981		
CT				0.274				-0.307	-0.306		
	R1-E	**R2b**	**R3**	**TS1b-E**	**I1b-E**	**I1'b-E**	**I2b-E**	**TS2b-E**	**TS2'b-E**	**Pb-E**	**P'b-E**
q_{C5}	-0.020			-0.137	-0.418	-0.423	-0.118	-0.009	-0.012	-0.129	-0.122
q_{C6}	-0.020			-0.057	-0.009	-0.069	-0.410	-0.389	-0.387	-0.094	-0.050
q_{C11}		0.257		0.406	0.623	0.655	0.657	0.690	0.691	-0.164	0.570
q_{N12}		-0.549		-0.448	-0.328	-0.332	-0.303	-0.270	-0.269	2.362	-0.476
q_{C14}			0.821				0.835	0.756		0.640	
q_{O15}			-0.530				-0.566			-0.632	
CT				0.273				-0.306	-0.308		
	R1-T	**R2b**	**R3**	**TS1b-T**	**I1b-T**	**I1'b-T**	**I2b-T**	**TS2b-T**	**TS2'b-T**	**Pb-T**	**P'b-T**
q_{C5}	-0.019			-0.125	-0.417	-0.416	-0.108	-0.001	-0.010	-0.317	-0.116
q_{C6}	-0.022			-0.063	-0.006	-0.064	-0.405	-0.387	-0.381	-1.009	-0.050
q_{C11}		0.258		0.409	0.626	0.655	0.657	0.692	0.693	1.090	0.566
q_{N12}		-0.549		-0.451	-0.332	-0.337	-0.308	-0.274	-0.275	-0.894	-0.494
q_{C14}			0.821				0.834	0.755		0.572	
q_{O15}			-0.530				-0.564	-0.694		-0.872	
CT				0.273				-0.308	-0.312		

Studies revealed that the atomic charge of N12 in R2b is slightly more than R2a while the significant variation of charge in C11 atom does not occur in these two structures. These results suggest that the more negative charge of N12 in R2b structure is related to the higher electron donor characteristics of di-*tert*-butyl compared to cyclohexyl. In the nucleophilic attack of R2 to R1, electronic charge is transferred from C11 to C6 and C5 atoms. Results show that the amount of electron density reduction in C11 and increase in the electron density of C5 and C6 atoms in all transition state structures (TS1a-M, TS1a-E, TS1b-M, TS1b-E and TS1b-T) are the same. More detailed studies indicate that charge density of C6 is more than C5. From AIM analysis, the electron density $\rho(r)$ of C6-C5 in transition state structures encountered with almost similar reduction with respect to the reactants (in the presence of various substituted groups). As expected, by decreasing the electron density of C11, the electron density of N12

also reduces. The main reason for charge reduction of C11 in the transition state structures is significant and important transition of LPC11→BD* (C5-C6). Formation of transition state structures is accompanied by formation of hydrogen bonds of C-H…O. The density of electrons in structures consisting two hydrogen bonds (TS1b-M and TS1b-E) are almost the same. Along with C11-C6 bond formation in the intermediate structure, the density of electrons in atom C11 diminishes and at the same time, the electron density of C5 reduced significantly, while the density of electrons for C6 slightly decreases. Association of negative charge on C5 atom is significantly higher than C6 atom. When the density of electrons in C11 decreases in the intermediate structure compared to transition state structures, the density of electrons in N12 also dwindles. C-H…O hydrogen bonds in intermediate structures also appear and the number of these bonds in all intermediate structures are equal. Comparing the density of electrons in these bonds illustrates a reduction in its value and the strength of the hydrogen bond with respect to the transition state structures. In I2a-M structure with high associated charge on C5 atom, a proper opportunity for the nucleophilic attack to the carbonyl group (C14-O15) is provided. This nucleophilic attack in the structure of TS2a-M is accompanied by a reduction of the density of electrons of C5 atom and an increase in the electron density of C14 atom. Presence of energy electron transfer (C14-O15) LPC5→BD* with high value of 101.88 kcal/mol suggests that the density of electrons in the C14-O15 bond is reduced. The obtained results also confirm these phenomena. It seems that O15-C11 bond formation resulting from nucleophilic attack of O15 atom to C11 atom occurs in TS2a-M structure, but more detailed investigations reveals that unexpectedly the density of electrons in C11 atom reduced and the electron density of O15 increases. Increasing of the electron density of O15 atom can be due to the higher polarity of the C14-O15 bond in nucleophilic attack of C5 atom, but the reduction of the electron density in C1 which is attacked by a nucleophilic process is not logical. Results of AIM analysis perfectly indicate that this interaction (C11-O15) in TS2a-M is an electrostatic interaction. The results also show that the nucleophilic attack of C5 to C14 atom provides the necessary driving force for the formation of transition state and ultimately the product. According to AIM analysis results, the final product (Pa-M) converts from electrostatic interaction C11-O15 to a strong covalent bond, this bond is stronger than the C5-C14 covalent bond. Formation of this bond in Pa-M results in a significant reduction of electron density of O15 atom and electron density of C11 atom. Moreover, the important transfer of LPO15→BD*(C11-N12) with energy of 32.61 kcal/mol induces a decrease in the electronic density of C11-N12 bond and associates charge on N12 atom. Monitoring the reaction in the presence of DAAD and isocyanide with different substitutions, illustrates that the obtained product from reaction between TBIC and DAAD reactants (reaction of b-T category) have the highest non-stable potential energy levels. Also the potential energy levels of these structures

in the reactions of b-E category are more stable than the reactions of a-E category and the potential energy levels of the structures in b-E category reactions are more stable than the one in the a-M reaction category. Comparison of potential energy levels in the presence of different alkyl groups indicates that in reactions of categories **a** and **b**, presence of bulk alkyl groups will result in the instability of the potential energy levels. Alkyl groups are known as electron donor groups, the charge analysis in R2a and R2b structures shows that upon replacement of substituted *tert*-butyl with cyclohexyl in R2 structure, the electronic charge of N12 in R2a, increases from -0.053 to -0.0551. Furthermore, the charge analysis in DAAD illustrates that the charge of oxygen atoms O4 and O8 in carbonyl groups increases in transition from substituted methyl groups to *tert*-butyl. These results are assigned to the electron donor characteristics compared to cyclohexyl and also with respect to methyl and ethyl substituted groups. However, the electron donor properties of these groups affect the electronic charge of oxygen atoms, but the electronic charge of C6 and C5 atoms in the bond don't present any specific variations. Moreover, in R2a and R2b structures, the electronic charge of N12 atoms has considerable variation, while there is not any detectable variation of electronic charge in C11 atom in the reaction. Therefore, it is expected that the electron donor characteristics is not the main factor of the potential energy level variation in the reaction, but the spatial prevention of substituted groups is the main reason of the potential energy level variation of the participating structures in the reaction. Investigation of the charge transfer amounts in the transition state structures suggests that in TS1a-M, the charge transfer from isocyanide to dialkyl acetylene decarboxylate occurs with the value of 0.272 e. This value of charge transfer in other transition state structures like TS1a-E, TS1b-M, TS1b-E and TS1b-T remains unchanged. Charge transfer in TS2a-M, from intermediate I1a'-M to acetic anhydride (R3) is -0.309 e. This value of charge transfer in other transition state structures such as TS2a-E, TS2b-M, TS2b-E and TS2b-T is almost the same. This obtained result is due to the constancy of the electronic charge of the participating atoms in the reaction in the presence of various substituted groups. In TS2 structure, the charge transfer from intermediate I1' to R3 will be representative of the nucleophilic attack of C5 to C14 atom which was predicted before.

Calculation of reaction rate constant

The obtained results from the quantum calculations in gas phase and at the presence of different solvents (acetone and dichloromethane) illustrated that the first energy barrier was significantly higher than the second one. Therefore, in all cases (in the presence of different substitutions in gas and aqueous phase) the first step of the reaction will be the rate-limiting step. A simplified scheme reaction mechanism is demonstrated in Figure 7. Rewriting the rate equation for ultimate product:

$$rate = k_4[I2] \tag{1}$$

By applying the steady-state approximation for the concentration of intermediate I2, we will have:

$$[I2] = \frac{k_3[I1'][R3]}{k_4} \tag{2}$$

Using steady-state approximation for intermediate I1':

$$[I1'] = \frac{k_2[I1]}{k_3[R3]} \tag{3}$$

Using the Equations (1), (2) and (3), a final equation for the given reaction is obtained which only consists of the rate constant of the first step.

$$rate = k_1[R1][R2] \tag{4}$$

This rate constant is of the second order due to the bimolecular transition state in the first step of the reaction. Therefore, calculation of this rate constant will result in the total reaction rate constant which is reported Table 5, for the reaction in the presence of DMAD, DEAD and DTAD both in gas and aqueous phase in.

Table **5**. Rate constant *k* in the presence of DMAD, DEAD and DTAD reactants

	k (cm^3/molecule.S)		
Structure	**gas phase**	**Acetone**	**dichloromethane**
DMAD (a)	3.86 E-27		
DEAD (a)	2.91 E-28		
DMAD (b)	1.01 E-27	3.89 E-28	2.51 E-28
DEAD (b)	5.90 E-28		
DTAD (b)	5.82 E-29		

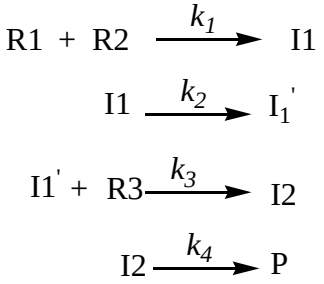

Figure 7. Simple schematic of the proposed mechanism for the reaction between R1, R2 and R3

Conclusions

The mechanistic investigation of the reaction among isocyanide, dialkyl acetylenedicarboxylate and acetic anhydride was undertaken. The potential competitive routes during the reaction coordinate were examined. Effect of solvent and substituted alkyl groups on the potential energy surfaces were investigated based upon the quantum mechanical calculations. Results are summarixed as bellow:

1. Results from quantum calculations indicated that different substituted groups in the structure of dialkyl acetylenedicarboxyalte and isocyanide do not cause any variation in the proposed mechanism of the reaction, but the potential energy levels encounter some variations which are not kinetically of high significance.
2. In the reaction between R2a and R1-M (R1-E) the potential energy levels of the obtained structures in the presence of R1-M, reduce compared to R1-E reactant. In addition, according to what can be concluded from the comparison of potential energy levels of the reaction between R2b and R1-M (R1-E and R1-T) reactants, it is demonstrated that the potential energy levels of the obtained structures were increased by going from R1-M to R1-T. The final products, in going from Pb-M (Pb'-M) to Pb-T (Pb'-T), are more unstable and more unspontaneous and the amount of exothermicity is reduced.
3. In all reaction paths, the rate-determining step is the first step of the reaction due to the higher energy barrier of the first step compared to the second step.
4. Total results indicate that dielectric effects of the solvent on the energy levels of the structures are more in dichloromethane, compared to acetone. The potential energy level in the presence of dichloromethane encountered an increase in most of the structures, but in the presence of acetone opposite behavior was observed.
5. Charge analysis of DAAD structure also illustrates that the charge of O4 and O8 atoms in carbonyl groups increased in going from substituting methyl groups to *tert*-butyl. Because of more electron donating effect. Although, the electron donating effect of these groups affect the electronic charge of oxygen atoms, but the electronic charge of C6 and C5 atoms do not represent any significant changes. Therefore, it is expected that the electron donating is not the main factor for the variation in the potential energy levels of the reaction, but the steric factor of bulky alkyl groups participating in the reaction path is the main factor of the variation in potential energy levels.

References

[1] Zangouei M., Esmaeili A.A., Habibi A., Fakhari A R. *Tetrahedron*., 2014, **70**:8619

[2] Banfi L., Basso A., Guanti G., Lecinska P., Riva R. *Mol. Div.,* 2008, **12**:187

[3] Ugi I., Meyer R., Fetzer U., Steinbruckner C. *Angew. Chem.,* 1959, **71**:386

[4] Baker R.H., Stanonis D. *J. Am. Chem. Soc.,* 1951, **73**:699

[5] Khan M.W., Alam M.J., Rashid M.A. *Bioorg. Med. Chem.,* 2005, **13**:4796

[6] Baharfar R., Baghbanian S.M. *Chin. Chem. Lett.,* 2012, **23**:677

[7] Yeung K.S., Yang Z., Peng X.S., Hou X.L. *Prog. Heterocycl. Chem.,* 2011, **22**:181

[8] Hamidi H., Heravi M.M., Tajbakhsh M., Shiri M., Oskooie H.A., Shintre S.A., Koorbanally N.A. *J. Iran. Chem. Soc.,* 2015, **12**:2205

[9] Haines N.R., VanZanten A.N., Cuneo A.A., Miller J.R., Andrews W.J., Carlson D.A., Harrington R.M., Kiefer A.M., Mason J.D., Pigza J.A., Murphree S.S. *J. Org. Chem.,* 2011, **76**:8131

[10] Yoshimura F., Sasaki M., Hattori I., Komatsu K., Sakai M., Tanino K., Miyashita M. *Chem. A Eur. J.,* 2009, **15**:6626

[11] Lee H.K., Chan K.F., Hui C.W., Yim H.K., Wu X.W., Wong H.N.C. *Pure Appl. Chem.,* 2005, **77**:139

[12] Montagnon T., Tofi M., Vassilikogiannakis G. *Acc. Chem. Res.,* 2008, **41**:1001

[13] Yu X., O'Doherty G., Chen X., Halcomb R. *De Novo Synthesis in Carbohydrate Chemistry*: From furans to Monosaccharides and oligosaccharides; ACS: Washington, 2008, p 3–22

[14] Gandini A., Silvestre A.J.D., Neto C.P., Sousa A.F., Gomes M. *Polym. Sci. A Polym. Chem.,* 2009, **47**:295

[15] Murphy E.B., Wudl F. *Prog. Polym. Sci.,* 2010, **35**:223

[16] Peart P.A., Tovar J.D. *Macromolecules*., 2009, **42**:4449

[17] Umeyama T., Takamatsu T., Tezuka N., Matano Y., Araki Y., Wada T., Yoshikawa O., Sagawa T., Yoshikawa S., Imahori H. *J. Phys. Chem.,* 2009, **113**:10798

[18] Wong N.H., Hou X.L., Yeung K.S., Huang H., Alvarez-Builla J. Modern Heterocyclic Chemistry; Wiley-VCH: Weinheim, 2011, p 533–592

[19] Sarvary A., Shaabani S., Shaabani A., Ng S.W. *Tetrahedron.,* 2011, **67**:3624

[20] Shaabani A., Rezayan A.H., Ghasemi S., Sarvary A. *Tetrahedron Lett.,* 2009, **50**:1456

[21] Frisch M.J., Trucks G.W., Schlegel H.B., Scuseria G.E., Robb M.A., Cheeseman J.R., Scalmani G., Barone V., Mennucci B., Petersson G.A., Nakatsuji H., Caricato M., Li X., Hratchian H.P., Izmaylov A.F., Bloino J., Zheng G., Sonnenberg J.L., Hada M., Ehara M., Toyota K., Fukuda R., Hasegawa J., Ishida M., Nakajima T., Honda Y., Kitao O., Nakai H., Vreven T., Montgomery J.A., Peralta J.E., Ogliaro F., Bearpark M., Heyd J.J., Brothers E., Kudin K.N., Staroverov V.N., Kobayashi R., Normand J., Raghavachari K., Rendell A., Burant J.C., Iyengar S.S., Tomasi J., Cossi M., Rega N., Millam J.M., Klene M., Knox J.E., Cross J.B., Bakken V., Adamo C., Jaramillo J., Gomperts R., Stratmann R.E., Yazyev O., Austin A.J., Cammi R., Pomelli C., Ochterski J.W., Martin R.L., Morokuma K., Zakrzewski V.G., Voth G.A., Salvador P., Dannenberg J.J. Dapprich S., Daniels A.D., Farka O., Foresman J.B., Ortiz J.V., Cioslowsk J., Fox D.J., Gaussian, Inc. Wallingford CT, 2009.

[22] Schmidt M.W., Baldridge K.K., Boatz J.A., Elbert S.T., Gordon M.S., Jensen J.H., Koseki S., Matsunaga N., Nguyen K.A., Su S., Windus T.L., Dupuis M., Montgomery J.A. *J Comput Chem*., 1993, **14**:1347

[23] Gonzalez C., Schlegel H.B. *J. Phys. Chem.,* 1990, **94**:5523

[24] Gonzalez C., Schlegel H.B. *J. Chem. Phys.,* 1989, **90**:2154

[25] Fukui K. *J. Phys. Chem.,* 1970, **74**:4161

[26] Fukui K. *Acc. Chem. Res.,* 1981, **14**:363

[27] Tomasi J., Persico M. *Chem. Rev.,* 1994, **94**:2027

[28] Cances E., Mennucci B., Tomasi J. *J. Chem. Phys.,* 1997, **107**:3032

[29] Cossi M., Barone V., Cammi R., Tomasi J. *Chem. Phys. Lett.,* 1996, **255**:327

[30] Glendening E.D., Reed A.E., Carpenter J.E., Weinhold F. NBO Version:3.1, 1998

[31] Biegler König F.W., Schönbohm. J, Bayles D. *J. Comput Chem*., 2001, **22**:545

How to cite this manuscript: Batoul Makiabadi, Mohammad Zakarianezhad*, Fahimeh Koorkinejad, Hoseyn Mehdizadeh, Theoretical Study of the Reaction Among Isocyanide, Dialkyl Acetylenedicarboxylate and Acetic Anhydride: The Investigation of the Reaction. Chemical Methodologies 4(4), 2020, 514-531. DOI:10.33945/SAMI/CHEMM.2020.4.11.